JOURNAL OF INFORMATION PROCESSING SYSTEMS JIPS

Detection of Microcalcification Using the Wavelet Based Adaptive Sigmoid Function and Neural Network

Sanjeev Kumar* and Mahesh Chandra*

Abstract

Mammogram images are sensitive in nature and even a minor change in the environment affects the quality of the images. Due to the lack of expert radiologists, it is difficult to interpret the mammogram images. In this paper an algorithm is proposed for a computer-aided diagnosis system, which is based on the wavelet based adaptive sigmoid function. The cascade feed-forward back propagation technique has been used for training and testing purposes. Due to the poor contrast in digital mammogram images it is difficult to process the images directly. Thus, the images were first processed using the wavelet based adaptive sigmoid function and then the suspicious regions were selected to extract the features. A combination of texture features and gray-level co-occurrence matrix features were extracted and used for training and testing purposes. The system was trained with 150 images, while a total 100 mammogram images were used for testing. A classification accuracy of more than 95% was obtained with our proposed method.

1. Introduction

Breast cancer is the leading cause of death in women and its death rate is only second to lung cancer. A recent study developed by the American Cancer Society [1] estimated at the end of 2013 that around 39,620 women die from breast cancer out of 232,340 women diagnosed with invasive breast cancer. Microcalcification and masses are two important early signs of breast cancer [2]. It is the most difficult to detect microcalcifications and masses because their features can be obscured. Since the causes of this disease still remain unknown, early detection is the only key solution to improve breast cancer prognosis. In this context, mammography has shown itself to be one of the most reliable methods for the early detection of breast cancer. Microcalcifications are deposits of calcium in breast tissue. Therefore, detecting calcifications in a mammogram is an important indicator for malignant breast disease. It is also present in many benign cases. The calcifications are generally small in size and they may be missed in the dense breast tissue. Sometimes calcifications have low contrast against the background and can be misinterpreted as noise in the heterogeneous background. In order to detect the

early onset of cancer in breast screening, it is essential to have high-quality images. The reading of mammogram images is a demanding job for radiologists and their judgements depend on their training and experience. Even an expert radiologist may have an inter-observe variation rate of 65%–75% [3]. CAD systems can improve a radiologist's performance by increasing the sensitivity rates as comparable to those obtained by radiologists, and in a cost effective manner. The combination of the CAD system and the knowledge of experts increases the cancer detection sensitivity rate by more than 90% [4].

The CAD system's first step is to convert the mammographic image to a digital mammogram image. After digitizing the mammogram images, it then carries out pre-processing. The main role of image pre-processing is to suppress noise and improve the contrast of the digital mammogram image. After that, the region of interest (ROI) is selected because the function of the ROI selection is to separate the suspicious regions from the normal region. The suspicious area is brighter than its surroundings. It has an almost uniform density and regular shape of suspicious region. The features of the different segments of an image are extracted and stored for training and testing purposes. The important features of a digital mammogram, such as size, shape, density, and smoothness of borders, can be calculated from the ROI's characteristics. The suspicious part of an image is detected by classifying the various segments of the image using the extracted features. Segmented parts of an image can be classified on the basis of normal tissues, benign masses, or malignant masses.

For pre-processing mammogram images many techniques are used for enhancing the contrast in digital mammograms. Generally, the digital mammograms are broken down into multiscale subband representation using the Contourlet transform [5] or different types of wavelet transforms [6-11]. After that, the transform coefficients in each subband of the multiscale representation are modified using different techniques, such as nonlinear filtering [12], regression-based extrapolation [13], adaptive unsharp masking [14], the wavelet shrinkage function [15], or direct contrast modification [16]. Finally, the enhanced digital mammograms can then be obtained from the modified coefficients.

However, it has been reported that a wavelet representation does not efficiently show the contours and the geometry of edges in images [5]. During the past few years the fuzzy set theory has also been used to enhance the contrast of digital mammograms since it is suitable for dealing with the uncertainty associated with the definition of mammogram edges, boundaries, and contrast [17-20]. However, the frequency domain techniques have certain limitations, such as artifacts called "objectionable blocking effects" [21], or it enhances images globally, but it does not enhance all of the local details/regions in the image very well. The enhancement techniques for digital mammograms in the spatial domain are based on nonlinear filtering [22,23] and with the human visual system (HVS) decomposition [24], adaptive neighborhood technique [19,25,26], or unsharp masking [27,28]. Ferrari et al. [29] and Rangayyan et al. [30] proposed a CAD system that is based on Gabor wavelets to detect the possibility of asymmetry. Yin et al. [31] proposed a method that automatically analyzes a pair of mammogram images and provides the result for the detection of asymmetric present in the image by applying direct methods and by using some alignment techniques. Some CAD systems are based on shape features [32,33]. Petrick et al. [32] used area measures, circular measures, convexity, rectangularity, perimeter, and perimeter to area ratio. Rangayyan et al. [33] used mean, variance, skewness, and kurtosis features. Some CAD systems are based on texture features [34]. The texture features, such as contrast, angular second moment entropy, and mean, are extracted from the gray level difference statistics vector of an image.

In this paper, the combination of texture features and grey level co-occurrence matrix (GLCM) features are used. Before feature extraction pre-processing was done by using the wavelet based adaptive

sigmoid function. The proposed CAD system requires less processing time and gives better accuracy for finding the microcalcifications and masses.

The rest of this paper is further organized into two sections. Section 2 is divided into two parts. The first part describes the pre-processing of mammogram images and the second part explains the cropping of images and features selection from the cropped images. Training and testing is also given in this section. Section 3 provides the conclusion and future work.

2. Proposed Method

The main focus of this work is to propose a new CAD system. In this system a wavelet based adaptive sigmoid function is used for pre-processing. The processing time and other features of our system are better than the previous existing methods. In this paper we use a combination of texture features and GLCM features. After training and testing, the performance of the proposed system has been found to be better than the performance of existing algorithms. The block diagram of the proposed CAD system is shown in Fig. 1(a) and (b).
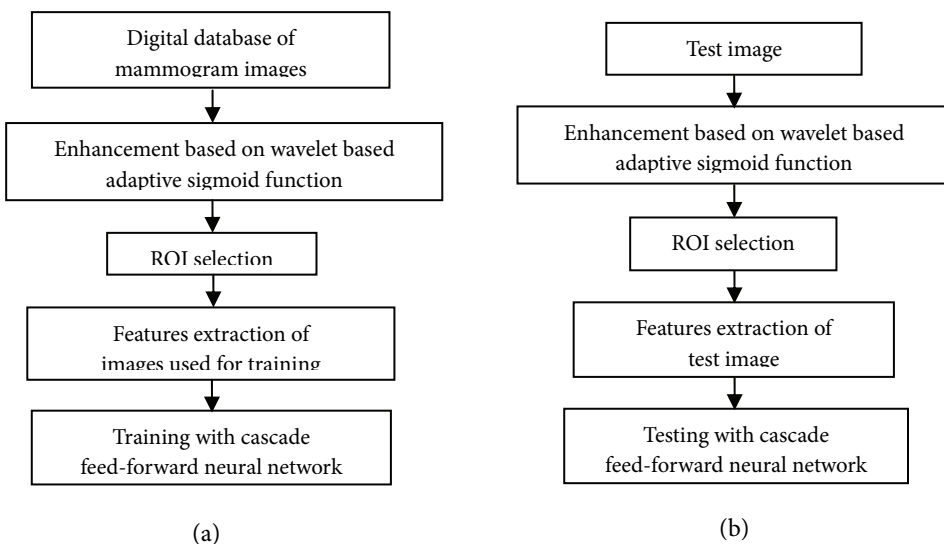

Fig. 1. Block diagram of the proposed CAD system. (a) Training system and (b) testing system.

2.1 Pre-processing

Since the contrast of digital mammogram images is low, it is necessary to improve the quality of the image by pre-processing it. The digital mammogram images are pre-processed by using the wavelet based adaptive modified sigmoid function (WBAMSF) [35]. The pre-processing of digital mammogram images consists of the following three steps: in the first step wavelet decomposition is done. In the second step the output image is processed by using the variable gain modified sigmoid function and in the third stage, the image is processed by adaptive histogram equalization. The block diagram of our proposed algorithm is shown in Fig. 2.
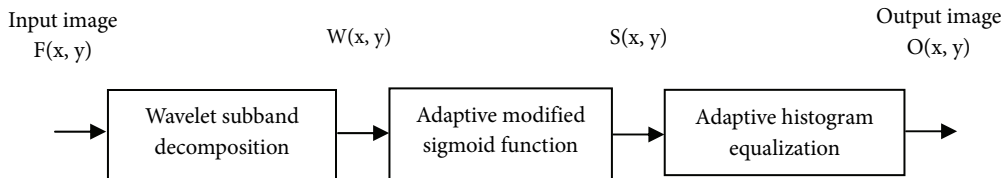
Input image
F(x, y)

W(x, y)

S(x, y)

Output image
O(x, y)

| Wavelet subband decomposition | Adaptive modified sigmoid function | Adaptive histogram equalization |

Fig. 2. Block diagram of proposed algorithm.

First Stage: A two-dimensional discrete wavelet transform provides a frequency band decomposition of the image where each subband can be quantized according to its visual importance. The two methods of convolution and lifting are used to apply a discrete wavelet transform, which leads to identical results. The convolution approach uses low pass and high pass filters. These two filters are called the analysis filter bank. The inverse discrete wavelet transform also utilizes two filters, which are called synthesis filter banks.

Second Stage: The sigmoid function is a non-linear continuous function. The name 'sigmoid' is derived from the 'S' shape of the function. Mathematically, the sigmoid function is defined by:

$$f(x) = \frac{1}{1 + e^{-\left(\frac{x-\alpha}{\beta}\right)}} \tag{1}$$

This function maps the entire range of x to the domain $[0, 1]$ of $f(x)$. The parameters α and β determine the center and width of the sigmoid function, respectively. Lal and Chandra [36] has used the sigmoid function for contrast enhancement with fixed gain parameters. Due to the fixed gain parameters only some of the images are enhanced in a better way, but not all of the images are. Here, the adaptive modified sigmoid function is being used where the gain parameters are not fixed. The adaptive modified sigmoid function is defined in Eq. (2). This mathematical formula operates upon pixel by pixel on an original image in the spatial domain. The pixel value of the second step output image is changed according to:

$$O(x, y) = F(x, y) + G_1 * \frac{F(x,y)}{1 - exp\,(G_1*(G_2 + F(x,y)))} \tag{2}$$

Where G_1 & G_2 are the variable gain of the input image and are given as:

G_1=mean (mean [original image])

G_2=sqrt (G_1)

The flow chart of this algorithm is shown in Fig. 3.

Third stage: The output of the processed image from the second stage is further processed by using the adaptive histogram equalization technique. The adaptive method computes several histograms, each of which corresponds to a distinct section of the image, and uses them to redistribute the brightness values of the image, which is different than ordinary histogram equalization. Therefore, it is more suitable for improving the local contrast of an image.

This section provides the simulation and experimental results of our proposed WBAMSF algorithm and other existing methods for the purpose of enhancing the contrast of digital mammogram images. The image quality parameters and subjective enhancement quality of our proposed WBAMSF method

was compared against four existing enhancement methods. The performance of each method is determined by the consistency of the measured results and the subjective evaluation of visual quality of mammograms.
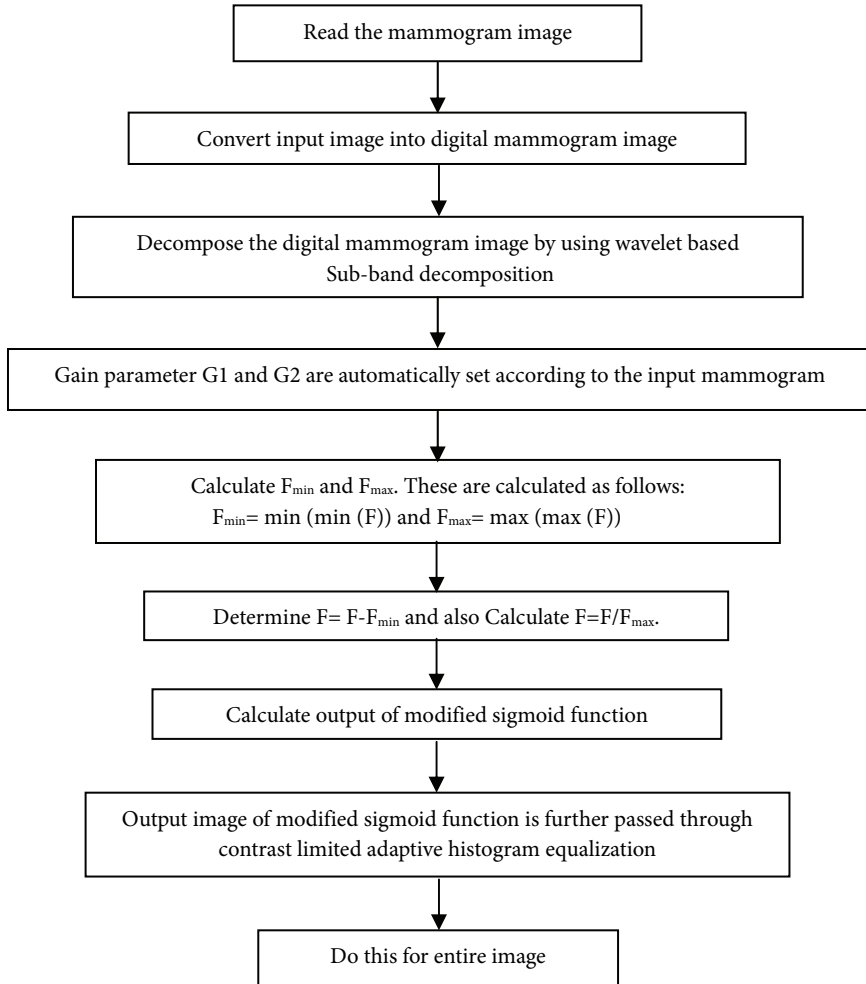
```
┌─────────────────────────────────────────┐
│        Read the mammogram image         │
└─────────────────────────────────────────┘
                    │
                    ▼
┌─────────────────────────────────────────────┐
│  Convert input image into digital mammogram  │
│                   image                       │
└─────────────────────────────────────────────┘
                    │
                    ▼
┌───────────────────────────────────────────────────┐
│ Decompose the digital mammogram image by using     │
│         wavelet based Sub-band decomposition        │
└───────────────────────────────────────────────────┘
                    │
                    ▼
┌──────────────────────────────────────────────────────┐
│ Gain parameter G1 and G2 are automatically set        │
│          according to the input mammogram             │
└──────────────────────────────────────────────────────┘
                    │
                    ▼
┌──────────────────────────────────────────────────────┐
│ Calculate Fmin and Fmax. These are calculated as      │
│ follows: Fmin= min (min (F)) and Fmax= max (max (F))  │
└──────────────────────────────────────────────────────┘
                    │
                    ▼
┌──────────────────────────────────────────────────────┐
│ Determine F= F-Fmin and also Calculate F=F/Fmax.      │
└──────────────────────────────────────────────────────┘
                    │
                    ▼
┌──────────────────────────────────────────────────────┐
│   Calculate output of modified sigmoid function       │
└──────────────────────────────────────────────────────┘
                    │
                    ▼
┌──────────────────────────────────────────────────────┐
│ Output image of modified sigmoid function is further  │
│ passed through contrast limited adaptive histogram    │
│                    equalization                       │
└──────────────────────────────────────────────────────┘
                    │
                    ▼
┌──────────────────────────────────────────────────────┐
│              Do this for entire image                 │
└──────────────────────────────────────────────────────┘
```

Fig. 3. Flow chart for pre-processing.

The measurement of the enhancement (EME) [37] of image $I(i, j)$ with dimensions $M_1 \times M_2$ pixels is defined as:

$$EME_{k_1 k_2} = \frac{1}{k_1 k_2} \sum_{l=1}^{k_1} \sum_{k=1}^{k_2} \left[20 * ln \left(\frac{I_{max,k,l}}{I_{min,k,l}} \right) \right] \tag{3}$$

where an image (I) is divided into $k_1 \times k_2$ blocks and, $I_{max,k,l}$,, $I_{min,k,l}$ are the maximum and minimum values of the pixels in each block.

The measure of enhancement factor (EMF) [37] between the output image and input image is defined as:

$$EMF = \frac{EME \ of \ output \ image}{EME \ of \ input \ image} \tag{4}$$

**Table 1.** Comparative performance of different methods for mammogram images

Parameter	AR	MSF	CLAHE	Adaptive histogram	WBAMSF (proposed)
mdb013.pgm					
EME (original)	1.92	1.92	1.92	1.92	1.92
EME (output)	2.03	4.27	4.53	4.53	6.22
EMF	1.06	2.22	2.36	2.38	3.23
CPU time (s)	0.78	0.36	0.16	0.32	0.13
mdb069.pgm					
EME (original)	3.72	3.72	3.72	3.72	3.72
EME (output)	3.81	6.56	6.56	3.81	8.57
EMF	1.02	1.76	1.76	1.02	2.30
CPU time (s)	0.92	0.36	0.17	0.81	0.15
mdb209.pgm					
EME (original)	3.63	3.63	3.63	3.63	3.63
EME (output)	3.69	5.21	7.35	7.35	9.35
EMF	1.01	1.43	2.02	2.02	2.57
CPU time (s)	0.88	0.37	0.18	0.36	0.12
mdb214.pgm					
EME (original)	2.36	2.36	2.36	2.36	2.36
EME (output)	2.44	2.24	3.08	3.08	5.32
EMF	1.04	0.95	1.31	1.31	2.25
CPU time (s)	0.81	0.33	0.16	0.31	0.12

AR=alpha rooting, MSF=modified sigmoid function, CLAHE=contrast limited adaptive histogram equalization, WBAMSF=wavelet based adaptive modified sigmoid function, EME=measurement of the enhancement, EMF= measure of enhancement factor.

Table 1 shows the comparative performance of different enhancement methods. In our experiment four MIAS database images mdb013.pgm, mdb069.pgm, mdb209.pgm, and mdb214.pgm were compared. Our proposed method was also tested with different images from the MIAS database. It can be noticed from Table 1 that the proposed method provides better qualitative results as compared to other existing algorithms, such as the alpha rooting (AR) algorithm, the modified sigmoid function (MSF), the contrast limited adaptive histogram equalization (CLAHE) algorithm, and the adaptive histogram. The Figs. 4(a) and 5(a) are the original mammogram images and Figs. 4(b) and 5(b) are the images that were processed with the proposed algorithm. As seen in Figs. 4(b) to 5(b) it is clear that the visual quality of the processed image is better and can be used for image segmentation.
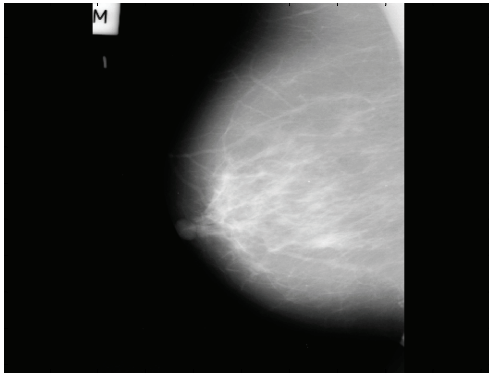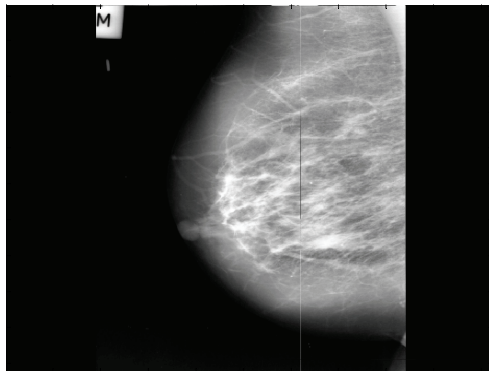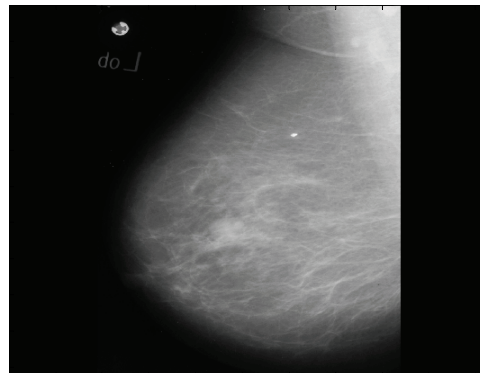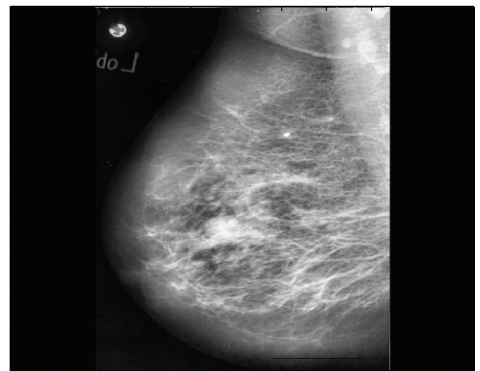
Fig. 4. (a) Original mdb013 and (b) processed image by proposed method.

Fig. 5. (a) Original mdb069 and (b) processed image by proposed method.

2.2 Feature Extraction and Simulation Results

After the digital image is pre-processed, the ROI is selected. The ROI is cropped from the original image for further processing. The 60x60 size images are then taken for further processing. After ROI selection, feature extraction and selection are done with a computer-aided diagnosis. These features are calculated for ROI. The feature space is very large and complex in nature due to its wide diversity of normal or abnormal tissues. By using a large number of features the performance of the algorithm may decrease or increase. Thus, useful feature extraction and selection is very important for better performance. The selection of ROI features is the process of selecting an optimum subset of features from the enormous amount of features available. The features are classified as: (a) intensity features, (b) geometric features, and (c) texture features.

We used a total of 13 combined features of texture and GLCM. These features are the perimeter, entropy, mean value, skew mean, eccentricity, extent value, major axis length, minor axis length, standard deviation, contrast, homogeneity, energy, and correlation. A brief description of some of the features is given below.

The perimeter 'p' is the distance around the boundary of the region. It computes the perimeter by calculating the distance between each adjoin pair of pixels around the border of the region. The mean value estimates the value of the image in which central clustering occurs. It is defined as:

$$\mu = \frac{1}{MN} \sum_{x=1}^{M} \sum_{y=1}^{N} p(x,y) \qquad (5)$$

where $p(x,y)$ is the pixel value at the point of an image of size $M \times N$.

The standard deviation σ is the estimate of the mean square deviation of gray pixel value $p(x,y)$ from its mean value. Mathematically, it is defined as:

$$\sigma = \sqrt{\frac{1}{MN} \sum_{x=1}^{M} \sum_{y=1}^{N} (p(x,y) - \mu)^2} \qquad (6)$$

The entropy 'h' is a statistical measure of randomness that can be used to characterize the texture of the input image. Mathematically, it is defined as:

$$h = -\sum_{k=0}^{L-1} p_{rk} (\log_2 p_{rk}) \qquad (7)$$

where p_{rk} is the probability of the k_{th} grey level, which can be calculated as $\frac{Z^k}{MxN}$, Z_k is the total number of pixels with the k_{th} grey level and 'L' is the total number of grey levels.

The energy 'E' is the sum of the squared elements in the GLCM. The range of energy is (0, 1) and the energy is 1 for a contrast image. Mathematically, it is defined as:

$$E = \sum_{x,y}^{M,N} p(x,y)^2 \qquad (8)$$

The contrast 'C' is the measure of the intensity between a pixel and its neighbor throughout the entire image. Mathematically, it is defined as:

$$C = \sum_{x,y}^{M,N} |x - y|^2 p(x,y) \qquad (9)$$

The correlation (Corr) is defined as the measure of pixel correlation to its neighbor throughout the entire image. The range of correlation is [-1, 1] and the correlation is 1 or -1 for a perfect positively or negatively correlated image. For a contrast image correlation is defined as:

$$\text{Corr} = \sum_{x,y}^{M,N} \frac{(x - \mu_x)(y - \mu_y)p(x,y)}{(\sigma_x \sigma_y)} \qquad (10)$$

where μ_x, μ_y, σ_x and σ_y are the measure of the means and standard deviation of p_x & p_y which are the partial probability density functions.

The homogeneity 'H' is a value that measures the closeness of the distribution of elements in the GLCM. The homogeneity values lie between [0, 1] and its value is 1 for the diagonal GLCM. Mathematically, it is defined as:

$$H = \sum_{x,y}^{M,N} \frac{p(x,y)}{1 + |x - y|} \qquad (11)$$

The skewness 'S' is the degree of the asymmetry of the pixel distribution in the specified window around its mean. Mathematically, it defined as:

$$S = \frac{1}{MN} \sum_{x,y}^{M,N} \left[\frac{p(x,y) - \mu}{\sigma} \right]^3 \qquad (12)$$

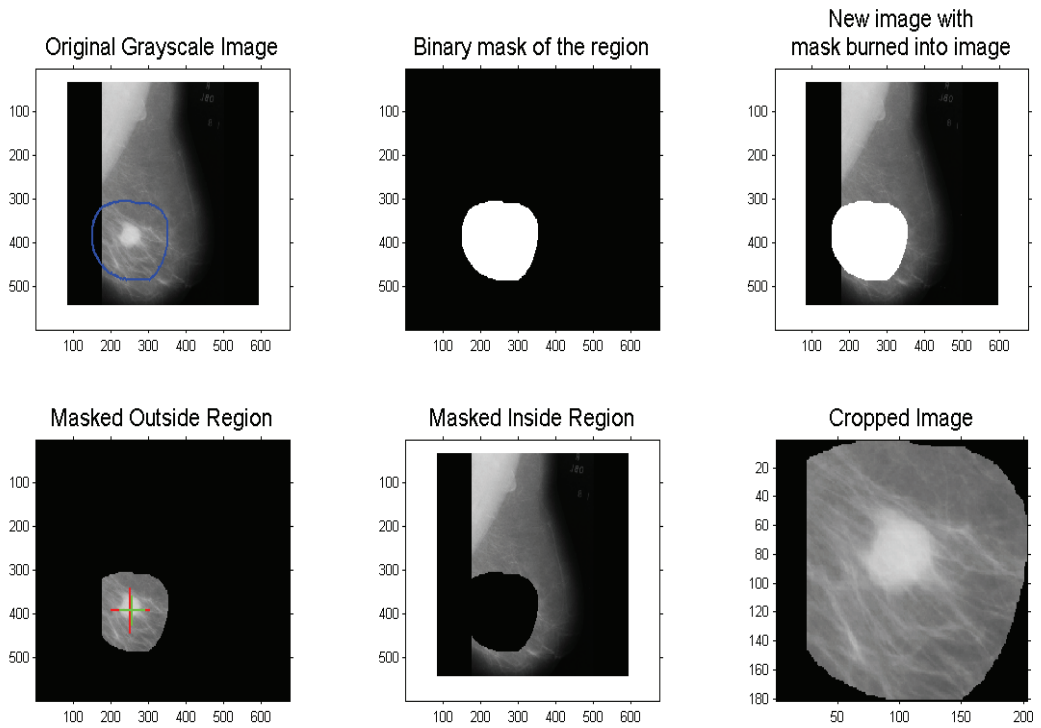where $p(x, y)$ is the pixel value at point (x, y) and μ & σ are the mean and standard deviation, respectively.
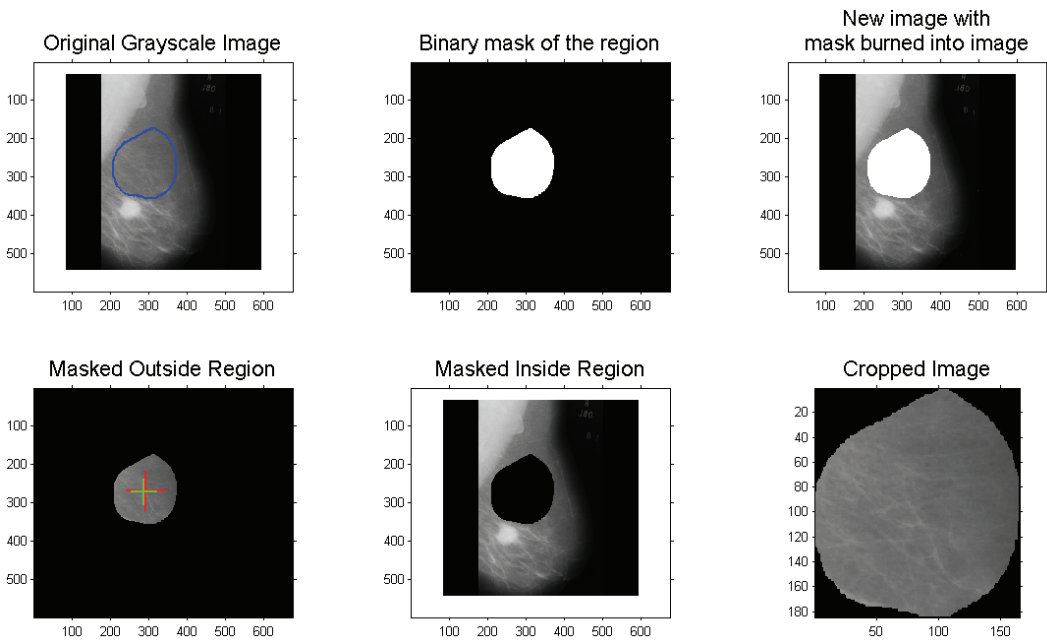

Fig. 6. Processing of image mdb028.

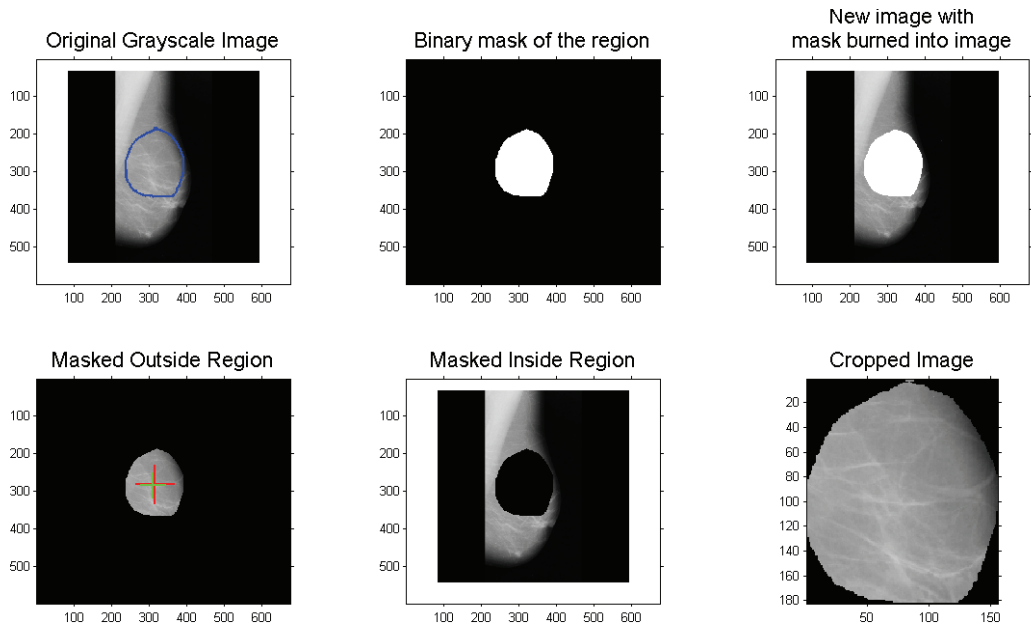**Fig. 7.** Processing of other part of image mdb028.

Fig. 8. Processing of image mdb080.

For training purposes 150 images were used. First, the image was cropped, as show in Figs. 6-9. The cropped image was then taken for further processing. A 60×60 image was taken from a cropped image, as shown in Figs. 10-13. The features of these cropped images are then calculated and stored. The cascade feed-forward back propagation technique was used for training purposes. In this case, we used 13 inputs and four hidden layers. For testing, the features were extracted similarly as was done for training.
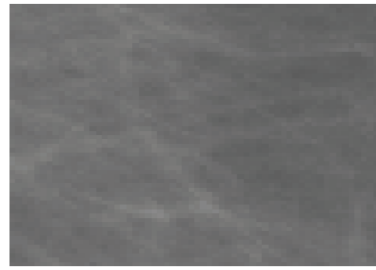
Fig. 9. Cropped image of Fig 6.

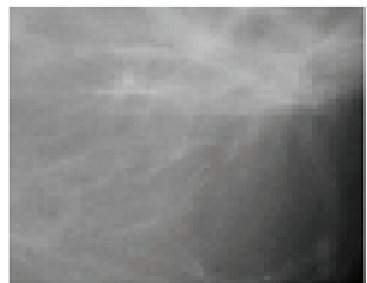**Fig. 10.** Cropped image of Fig 7.
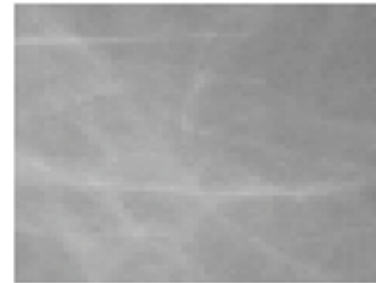
Fig. 11. Cropped image of Fig 8.

Fig. 12. Cropped image of Fig 9.

Figs. 6 and 7 are from different parts of the same image. Similarly, Figs. 8 and 9 are also from different parts of the same image. Figs. 6 and 7 show the processing of image mdb028, Fig. 6 contains the affected part, and Fig. 7 contains the unaffected part. After testing the exact location of the normal part and the affected parts can be determined. Similarly, Figs. 8 and 9 are from the same image mdb080 and in both, the selected part contains the affected parts. This process was applied to different images to find the exact location of the affected part.

3. Conclusion

Our proposed method provides better performance in comparison to other existing algorithms. For this method, we used a wavelet based adaptive sigmoid algorithm for pre-processing and it takes less time to process images. Comparative studies on contrast enhancement the fact that the proposed features perform better than existing algorithms. Training and testing was carried out by using both GLCM and texture features with the cascade-forward back propagation technique. In this case, the abnormality can be found anywhere in an image by selecting and checking of suspicious region. In the future, hybrid features or different types of image features can be used to achieve better results.

References

[1] American Cancer Society, "Cancer facts & figures 2013," http://www.cancer.org/acs/groups/content/ @epidemiologysurveilance/documents/document/acspc-036845.pdf.

[2] H. D. Cheng, X. Cai, X. Chen, L. Hu, and X. Lou, "Computer-aided detection and classification of microcalcifications in mammograms: a survey," *Pattern Recognition*, vol. 36, no. 12, pp. 2967-2991, 2003.

[3] P. Skaane, K. Engedal, and A. Skjennald, "Interobserver variation in the interpretation of breast imaging: comparison of mammography, ultrasonography, and both combined in the interpretation of palpable noncalcified breast masses," *Acta Radiologica*, vol. 38, no. 4, pp. 497-502, 1997.

[4] M. Kallergi, K. Woods, L. P. Clarke, W. Qian, and R. A. Clark, "Image segmentation in digital mammography: comparison of local thresholding and region growing algorithms," *Computerized Medical Imaging and Graphics*, vol. 16, no. 5, pp. 323-331, 1992.

[5] Z. Lu, T. Jiang, G. Hu, and X. Wang, "Contourlet based mammographic image enhancement," in *Proceedings of SPIE 6534: Fifth International Conference on Photonics and Imaging in Biology and Medicine.* Bellingham, WA: International Society for Optics and Photonics, 2007, pp. 65340M-65340M.

[6] A. Laine, J. Fan, and W. Yang, "Wavelets for contrast enhancement of digital mammography," *IEEE Engineering in Medicine and Biology Magazine*, vol. 14, no. 5, pp. 536-550, 1995.

[7] A. Laine, S. Schuler, J. Fan, and W. Huda, "Mammographic feature enhancement by multiscale analysis," *IEEE Transactions on Medical Imaging*, vol. 13, no. 4, pp. 725-74, 1994.

[8] A. Mencattini, M. Salmeri, R. Lojacono, M. Frigerio, and F. Caselli, "Mammographic images enhancement and denoising for breast cancer detection using dyadic wavelet processing," *IEEE Transactions on Instrumentation and Measurement*, vol. 57, no. 7, pp. 1422-1430, 2008.

[9] P. Sakellaropoulos, L. Costaridou, and S. Panayiotakis, "A wavelet-based spatially adaptive method for mammographic contrast enhancement," *Physics in Medicine and Biology*, vol. 48, no. 6, pp. 787-803, 2003.

[10] P. Heinlein, J. Drexl, and W. Schneider, "Integrated wavelets for enhancement of microcalcifications in digital mammography," *IEEE Transactions on Medical Imaging*, vol. 22, no. 3, pp. 402-413, 2003.

[11] S. Skiadopoulos, A. Karahaliou, F. Sakellaropoulos, G. Panayiotakis, and L. Costaridou, "Breast component adaptive wavelet enhancement for soft-copy display of mammograms," in *Digital Mammography.* Heidelberg: Springer, 2006. pp. 549-556.

[12] C. M. Chang and A. Laine, "Coherence of multiscale features for enhancement of digital mammograms," *IEEE Transactions on Information Technology in Biomedicine*, vol. 3, no. 1, pp. 32-46, 1999.

[13] G. Derado, F. D. Bowman, R. Patel, M. Newell, and B. Vidakovic, "Wavelet image interpolation (WII): a wavelet-based approach to enhancement of digital mammography images," in *Proceedings of the 3rd Symposium on Bioinformatics Research and Applications (ISBRA)*, Atlanta, GA, 2007, pp. 203-214.

[14] F. Y. Lure, P. W. Jones, and R. S. Gaborski, "Multiresolution unsharp masking technique for mammogram image enhancement," in *Proceedings of SPIE 2710: Medical Imaging 1996.* Bellingham, WA: International Society for Optics and Photonics, 1996, pp. 830-839.

[15] J. Scharcanski and C. R. Jung, "Denoising and enhancing digital mammographic images for visual screening," *Computerized Medical Imaging and Graphics*, vol. 30, no. 4, pp. 243-254, 2006.

[16] J. Tang, X. Liu, and Q. Sun, "A direct image contrast enhancement algorithm in the wavelet domain for screening mammograms," *IEEE Journal of Selected Topics in Signal Processing*, vol. 3, no. 1, pp. 74-80, 2009.

[17] H. D. Cheng and H. Xu, "A novel fuzzy logic approach to mammogram contrast enhancement," *Information Sciences*, vol. 148, no. 1, pp. 167-184, 2002.

[18] F. Sahba and A. Venetsanopoulos, "Contrast enhancement of mammography images using a fuzzy approach," in *Proceedings of the 30th Annual International Conference of the IEEE Engineering in Medicine and Biology Society (EMBS2008)*, Vancouver, Canada, 2008, pp. 2201-2204.

[19] I. Stephanakis, G. Anastassopoulos, A. Karayiannakis, and C. Simopoulos, "Enhancement of medical images using a fuzzy model for segment dependent local equalization," in *Proceedings of the 3rd International Symposium on Image and Signal Processing and Analysis (ISPA2003)*, Rome, Italy, 2003, pp. 970-975.

[20] J. Jiang, B. Yao, and A. M. Wason, "Integration of fuzzy logic and structure tensor towards mammogram contrast enhancement," *Computerized Medical Imaging and Graphics*, vol. 29, no. 1, pp. 83-90, 2005.

[21] S. Aghagolzadeh and O. K. Ersoy, "Transform image enhancement," *Optical Engineering*, vol. 31, no. 3, pp. 614-626, 1992.

[22] N. Petrick, H. P. Chan, B. Sahiner, and D. Wei, "An adaptive density-weighted contrast enhancement filter for mammographic breast mass detection," *IEEE Transactions on Medical Imaging*, vol. 15, no. 1, pp. 59-67, 1996.

[23] W. Qian, L. P. Clarke, M. Kallergi, and R. Clark, "Tree-structured nonlinear filters in digital mammography," *IEEE Transactions on Medical Imaging*, vol. 13, no. 1, pp. 25-36, 1994.

[24] Y. Zhou, K. Panetta, and S. Agaian, "Human visual system based mammogram enhancement and analysis," in *Proceedings of 2010 2nd International Conference on Image Processing Theory Tools and Applications (IPTA)*, Paris, France, 2010, pp. 229-234.

[25] A. P. Dhawan, G. Buelloni, and R. Gordon, "Enhancement of mammographic features by optimal adaptive neighborhood image processing," *IEEE Transactions on Medical Imaging*, vol. 5, no. 1, pp. 8-15, 1986.

[26] V. H. Guis, M. Adel, M. Rasigni, G. Rasigni, B. Se, and P. Heid, "Adaptive neighborhood contrast enhancement in mammographic phantom images," *Optical Engineering*, vol. 42, no. 2, pp. 357-366, 2003.

[27] G. Ramponi, N. K. Strobel, S. K. Mitra, and T. H. Yu, "Nonlinear unsharp masking methods for image contrast enhancement," *Journal of Electronic Imaging*, vol. 5, no. 3, pp. 353-366, 1996.

[28] Z. Wu, J. Yuan, B. Lv, and X. Zheng, "Digital mammography image enhancement using improved unsharp masking approach," in *Proceedings 2010 3rd International Congress on Image and Signal Processing (CISP)*, Yantai, China, 2010, pp. 668-672.

[29] R. J. Ferrari, R. M. Rangayyan, and J. L. Desautels, "Analysis of asymmetry in mammograms via directional filtering with Gabor wavelets," *IEEE Transactions on Medical Imaging*, vol. 20, no. 9, pp. 953-964, 2010.

[30] R. M. Rangayyan, R. J. Ferrari, and A. F. Frere, "Analysis of bilateral asymmetry in mammograms using directional, morphological, and density features," *Journal of Electronic Imaging*, vol. 16, no. 1, article no. 013003, 2007.

[31] F. F. Yin, M. L. Giger, K. Doi, C. J. Vyborny, and R. A. Schmidt, "Computerized detection of masses in digital mammograms: automated alignment of breast images and its effect on bilateral-subtraction technique," *Medical Physics*, vol. 21, no. 3, pp. 445-452, 1994.

[32] N. Petrick, H. P. Chan, B. Sahiner, and M. A. Helvie, "Combined adaptive enhancement and region-growing segmentation of breast masses on digitized mammograms," *Medical Physics*, vol. 26, no. 8, pp. 1642-1654, 1999.

[33] R. M. Rangayyan, N. M. El-Faramawy, J. L. Desautels, and O. Alim, "Measures of acutance and shape for classification of breast tumors," *IEEE Transactions on Medical Imaging*, vol. 16, no. 6, pp. 799-810, 1997.

[34] B. Sahiner, H. P. Chan, N. Petrick, D. Wei, M. Helvie, D. D. Adler, and M. M. Goodsitt, "Classification of mass and normal breast tissue: a convolution neural network classifier with spatial domain and texture images," *IEEE Transactions on Medical Imaging*, vol. 15, no. 5, pp. 598-610, 1996.

[35] S. Kumar and M. Chandra, "An efficient method for contrast enhancement of digital mammographic images," in *Soft Computing Techniques in Engineering Applications*. Heidelberg: Springer, 2014, pp. 59-74.

[36] S. Lal and M. Chandra, "Efficient algorithm for contrast enhancement of natural images," *International Arab Journal of Information Technology*, vol. 11, no. 1, pp. 95-102, 2014.

[37] K. Panetta, Y. Zhou, S. Agaian, and H. Jia, "Nonlinear unsharp masking for mammogram enhancement," *IEEE Transactions on Information Technology in Biomedicine*, vol. 15, no. 6, pp. 918-928, 2011.

Sanjeev Kumar http://orcid.org/0000-0002-4662-288X

He received M.E. degree in Electronics & Communication from BIT MESRA, RANCHI, INDIA in 2012. He is perusing Ph.D. from BIT MESRA, RANCH, INDIA. His research interests are in the area of Image processing, Pattern Recognition, Multimedia Processing, Video/Audio Watermarking.

Mahesh Chandra http://orcid.org/0000-0001-9892-5527

He received A.M.I.E. from I.E.I., Kolkata, India in winter 1994. He received M.Tech. from J.N.T.U., Hyderabad in 2000 and Ph.D. from AMU, Aligarh in 2008. Presently, he is working as Associate Professor in the Department of Electronics & Communication Engineering at Birla institute of technology Mesra, Ranchi, India. He has published more than 115 research papers in the area of speech, signal and image processing at National/International levels. He has written one book on Dynamic Adaptive Filter Design-With Applications to Acoustic Echo and Noise Control. He has guided 07 Ph.D. students and 20 M. Tech students for their research work. He is a member of IEEE USA, ISTE India and Fellow of IETE, India. He has delivered a number of keynote talks and chaired many sessions.